Cross-Layer Optimal Policies for Spatial Diversity Relaying in Mobile Ad Hoc Networks

Jing Ai, *Student Member, IEEE*, Alhussein A. Abouzeid, *Member, IEEE*, and Zhenzhen Ye, *Student Member, IEEE*

***Abstract*— In order to adapt to time-varying wireless channels, various channel-adaptive schemes have been proposed to exploit inherent spatial diversity in mobile/wireless ad hoc networks where there are usually alternate next-hop relays available at a given forwarding node. However, current schemes along this line are designed based on heuristics, implying room for performance enhancement. To seek a theoretical foundation for improving spatial diversity gain, we formulate the selection of the next-hop as a sequential decision problem and propose a general "Optimal Stopping Relaying (OSR)" framework for designing such next-hop diversity schemes. As a particular example, assuming Rayleigh fading channels, we implement an OSR strategy to optimize information efficiency (IE) in a protocol stack consisting of Greedy Perimeter Stateless Routing (GPSR) and IEEE 802.11 MAC protocols. We present mathematical analysis of the proposed OSR together with other strategies in literature for a single forwarding node. In addition, we perform extensive simulations (using QualNet) to evaluate the end-to-end performance of these relaying strategies in a multi-hop network. Both the mathematical and simulation results demonstrate the superiority of OSR over other existing schemes.**

***Index Terms*— Mobile ad hoc networks, cross-layer design, spatial/next-hop diversity, optimal stopping, information efficiency.**

I. Introduction

WIRELESS ad hoc networks achieve greater geographic coverage and enhanced energy and spectral efficiency through multi-hop relaying, by which every packet is delivered to its destination along a path in a hop-by-hop fashion. However, most previous studies of forwarding/routing protocols ignore the time-varying nature of underlying wireless links due to multi-path fading and interference from other concurrent transmissions in the network. Thus, existing communication protocols for multi-hop routing suffer substantial performance degradation when operating in realistic environments.

In order to combat these adverse channel variation effects, recent works (e.g., [2]–[6]) exploit spatial diversity inherent in multi-hop wireless networks due to the presence of alternate next-hop relaying nodes. In a multiple candidate relays environment with mutually independent wireless links, it is highly probable that the channel condition at one of the candidate relays has a high signal-to-noise ratio (SNR). Notice that this next-hop diversity is in the same spirit of multiuser diversity rooted in [7].

Nevertheless, several design challenges must be first overcome so that we can take the advantage of the possible performance improvements due to this type of spatial diversity, particularly regarding the design of a strategy for selection of the next-hop, and the design of low overhead routing and MAC layers that jointly leverage the spatial diversity in the presence of rapid fluctuations in the quality of the channels. This is due to the fact that, since the channel approximately remains constant on the order of channel coherence time [8], acquiring valid channel state information (CSI) is relatively costly and channel probing overhead may negate the gains achieved by diversity. Thus, there exists a critical trade-off between the amount of information obtained from the physical/link layer and the quality of the selected next-hop relay (and hence the achieved spatial diversity gain).

Notice that current works in literature only explore two extreme cases. The forwarding node in [3], [4] initially sends a query to a set of candidate nodes, and the node which is able to respond first is selected as the next-hop relay. For convenience, we refer to this class of strategies as the *First Stopping Relaying (FSR)* scheme. While FSR has the advantage of inducing a short decision delay, its main drawback is that the extreme (min-delay) decision rule may result in missing a better channel. This may give rise to a higher channel outage probability or lower data rates especially when multi-rate radios are employed. On the other hand, the forwarding node in [5], [6] collects CSI from *all* candidate nodes and then makes the forwarding decision. We refer to this class of strategies as the *Last Stopping Relaying (LSR)* scheme. LSR selects "the best" relay based on full information collected on all relaying nodes. In return, its main drawback is that the extreme (max-overhead) decision rule may result in not only invalidation of the collected CSI by the time the forwarding node uses the selected channel, but also lower effective link throughput[1] on a per-packet basis. Therefore, it is natural to investigate whether a better trade-off could be achieved by combining the advantages of these two extremes, which we attempt to do here through a stochastic decision framework.

In this paper, we formulate the next-hop selection problem as a sequential decision problem and derive an Optimal Stopping Relaying (OSR) strategy that maximizes the average

Manuscript received July 17, 2006; revised February 7, 2007, September 30, 2007, and June 9, 2008; accepted June 23, 2008. The associate editor coordinating the review of this paper and approving it for publication was R. Berry. This paper was presented in part at the 2006 IEEE MASS Conference [1].

The authors are with the Department of Electrical, Computer and Systems Engineering, Rensselaer Polytechnic Institute, Troy, New York 12180 (e-mail: {aij, abouza, yez2}@rpi.edu).

Digital Object Identifier 10.1109/TWC.2008.060483.

[1]Effective link throughput means the fraction of link throughput used for user data transport.

reward, defined as a function related to the network performance. One of the practical advantages of this formulation is that, by only requiring long-term channel statistics, the forwarding node can calculate a threshold-based (and hence low complexity) policy based on optimal stopping theory (e.g., [9]) which guarantees the selected relay can optimize a customized performance metric. Equally important is the fact that a low-overhead implementation exists by conveying such a policy to the set of candidate relays, so that each candidate relay can decide whether it can be "the selected one" independently without explicitly feeding back the channel measurements (i.e., no exchange of channel states between the candidate relays and the forwarding node). In case more than one node qualifies under the policy, a priority-based scheme (e.g., [3], [4]) or a well studied splitting algorithm (e.g., [10]) can be used to ensure the desired relay in the original decision problem is selected within a short resolution delay.

The contribution of this paper is threefold. First, we propose a general framework, OSR, which can optimize an arbitrary channel-related metric locally and can be integrated with almost any MAC/routing protocol stack. Second, as a particular example, assuming Rayleigh fading channels, we implement OSR to optimize a generalized information efficiency (IE) (first defined in [11]) in a protocol stack composed of Greedy Perimeter Stateless Routing (GPSR) [12], [13] and IEEE 802.11 MAC protocols. Third, we analyze the forwarding capability of a single forwarding node and evaluate the end-to-end multi-hop performance via extensive simulations using QualNet [14]. Both of these results demonstrate the superiority of OSR over FSR and LSR.

The rest of the paper is organized as follows. The next section presents a general framework of OSR, followed by two sections that address its underlying optimal stopping theory and implementation in a stack of GPSR and IEEE 802.11 MAC protocols. In Section V, we analyze the forwarding capability of a single node for OSR, FSR and LSR in terms of the expected IE achieved. In Section VI, we further perform extensive simulations using QualNet to evaluate their end-to-end performance. Finally, Section VII concludes the paper.

II. Optimal Stopping Relaying Framework

In this section, we show how the next-hop selection problem can be formulated as a sequential decision problem that attains a better trade-off between the achieved spatial diversity gain and the cost induced by obtaining physical/link layer information from the next-hop candidate nodes. Notice that Multi-channel Opportunistic Auto-rate (MOAR) [15] comes closest to our work from the problem formulation standpoint. Their work is different in that their objective is to exploit *frequency* (rather than time) diversity with multi-channel radios (i.e., no forwarding nodes). However, it cannot be adapted to exploit spatial diversity studied in this paper because in MOAR: a) only identical and independently distributed (i.i.d.) channels are assumed; b) CSI from each candidate relay has to be acquired sequentially which may result in large channel acquisition time. When exploiting spatial diversity in OSR, we utilize the fact that it is possible to measure CSI simultaneously at multiple candidate relays by taking advantage of the broadcast nature of the wireless medium, which results in a shorter decision delay.

In this paper, we solve such a sequential decision problem based on optimal stopping theory which provides a solid theoretical foundation for designing such schemes. In conventional settings of an optimal stopping problem, a decision maker observes a sequence of random variables, given their joint probability distribution and associated real-valued reward functions. For each time step, after observing a random variable and calculating the obtained reward up to that point in time, the decision-maker takes an action to stop or continue the procedure in hope for a better reward. The goal of the problem is to derive an optimal policy in order to maximize the expected reward. In wireless ad hoc networks, this general framework requires collaboration among multiple protocol layers in a distributed manner as described below.

We assume a cross-layer framework whereby a node's physical layer overhears the channel and provides CSI to upper layers if necessary. Thereby, the MAC layer is able to maintain the long-term channel statistics for every neighbor it hears. When a node needs to forward a packet, the routing layer is first responsible to select a set of candidate relays according to the customized metric. Then, based on available information (i.e., the set of candidate nodes and related channel statistics) provided by PHY/MAC and routing layers, the node can calculate its optimal stopping policy. In order to minimize the delay and communication costs, our design opts to perform the policy *on the relay side*. The MAC layer multi-casts a polling message which carries the policy parameters to the set of candidate relays and each receiver can perform the policy to decide whether it is "the selected one" independently. Notice that, in a related work [16], a similar idea is used in order to amortize the cost of contention resolution, where a node multi-casts a batch of packets toward a set of candidate relays at a time and then makes the delayed forwarding decisions.

In case more than one node qualifies under the policy (we will discuss later how/if the policy will provide multiple results), there are several options to tackle the potential collisions and ensure the selection of the desired relay in the original decision problem within a short resolution delay. When the number of candidate nodes is small and collision detection cost is high, a priority-based scheme (e.g., [3], [4]) is used in which each response by a node is prioritized in time in an order specified in the polling message. When the number of candidate nodes is large and collision detection cost is low, a variant of the splitting algorithm (e.g., [10]) is used to filter out the desired relay via a tree-like mechanism.

III. Optimal Stopping Relaying Theory

A. Rayleigh Fading Channels

In order to understand the behavior of higher layer protocols or finely tune their parameters in wireless networks, it is common to assume that the underlying channel is a flat Rayleigh fading channel. This model captures the fading phenomenon when there is no predominant line-of-sight between a transmitter and receiver. Hence, in the presence of Rayleigh fading channels, the instantaneous SNR Γ conforms to an exponential distribution with probability density function

(PDF) $f(\gamma) = \frac{1}{\overline{\gamma}} e^{-\frac{\gamma}{\overline{\gamma}}},\ \gamma \geq 0$, where $\overline{\gamma} = E\{\Gamma\}$ is the average SNR.

In general, the evolution of Rayleigh fading channels can be modeled as a finite state Markov chain (FSMC) (e.g., see [17]). In an FSMC model, the SNR is partitioned into disjoint intervals and then mapped into a finite-state space $\mathcal{S} = \{s_1, s_2, \ldots, s_K\}$. Suppose that the SNR thresholds are $\vec{\gamma} = \{\gamma_1 = 0, \gamma_2, \ldots, \gamma_{K+1} = \infty\}$. If an instantaneous SNR Γ satisfies $\gamma_k \leq \Gamma < \gamma_{k+1}$, the channel is said to be in state k. Since the instantaneous channel SNR Γ conforms to an exponential distribution, then, when a node probes the channel, its steady-state probability of being in state s_k is given by

$$\pi_k = \int_{\gamma_k}^{\gamma_{k+1}} f(\gamma) d\gamma = e^{-\frac{\gamma_k}{\overline{\gamma}}} - e^{-\frac{\gamma_{k+1}}{\overline{\gamma}}},\ k = 1, 2, \ldots, K. \tag{1}$$

We here generalize the FSMC model [17], [18] to allow transitions between nonadjacent states to be able to capture fast fading channels. The transition probability from state s_k to state s_j after a time interval τ can be derived as (see Appendix for more details)

$$p(k, j, \tau) \approx \begin{cases} \frac{N(\gamma_j)}{\sum_{i=k}^{j-1} \pi_i} \frac{\pi_k}{\sum_{i=k}^{j-1} \pi_i} \tau & \text{if } j \geq k+1 \\ \frac{N(\gamma_{j+1})}{\sum_{i=j+1}^{k} \pi_i} \frac{\pi_k}{\sum_{i=j+1}^{k} \pi_i} \tau & \text{if } j \leq k-1 \\ 1 - \sum_{i \neq k} p(k, i, \tau) & \text{if } j = k \end{cases} \tag{2}$$

where $N(\gamma)$ is the level crossing rate (LCR) of level γ for the SNR process in either positive or negative direction, which can be estimated as [18, eq. (3)]

$$N(\gamma) = \sqrt{\frac{2\pi\gamma}{\bar{\gamma}}} f_m e^{-\frac{\gamma}{\bar{\gamma}}} \tag{3}$$

where f_m denotes the maximum Doppler frequency defined as $f_m = \frac{v_m}{\lambda}$ (v_m is the maximum fading velocity and λ is the carrier wavelength).

B. Reward Function

In literature, there are a number of metrics that have been used to select the next-hop relay. For example, in [19], [20], the node selects the relay that maximizes the progress of the packet toward the destination. In [3], [4], a node seeks the first qualified channel sequentially according to some predetermined preference list. In [21], a node attempts to maximize the IE, which balances the need to minimize the number of hops along a route with the need to maximize the throughput on a given hop.

In our proposed OSR scheme, we let the node select the relay based on a generalized IE Θ defined as follows:

$$\Theta = dR \tag{4}$$

where d denotes the distance progress made by the transmission toward the destination and R denotes the highest reliable data rate determined by the instantaneous channel SNR Γ at the candidate relay node. Without loss of generality (with respect to a multi-rate radio), we can specify a set of SNR thresholds in the above FSMC model so that each state is associated with a distinct data rate. Thus, the corresponding data rate denoted as R can be characterized as a discrete random variable with a probability mass function (PMF)

$$R = r_k \quad w.p.\ \pi_k\ , k = 1, 2, \ldots, K. \tag{5}$$

Notice that we set $r_1 = 0$ in state s_1 and thus γ_2 is the minimum SNR required by any effective reception. Since d can be considered as a constant at the time scale of forwarding a packet, Θ is a discrete random variable with the same PMF as R, given in (5).

Recall that, as mentioned in Section II, due to the need to resolve potential collisions when more than one relay are qualified, there may exist a certain delay between the time that the relay observes Θ and the time that the forwarding node actually forwards the packet to the selected relay. Such delay not only may degrade the quality of the observed channel but also may diminish the effective link throughput by a factor of $\frac{\tau_{DATA}}{\tau}$, where τ_{DATA} and τ are the transmission times without/with channel probing overheads of a data packet, respectively. Therefore, we define the reward function of the forwarding node as follows:

$$y_i(\theta_1, \theta_2, \ldots, \theta_i) = \theta_i \alpha(f(\frac{\theta_i}{d_i}), i),\ 1 \leq i \leq L \tag{6}$$

where $f(r_k)$ denotes the index of the data rate $r_k = \frac{\theta_i}{d_i}$($2 \leq k \leq K$), i denotes the index of selected candidate relay and $\alpha(k, i) (\in [0, 1])$, the discount factor given the i-th relay is selected in OSR, is defined as

$$\alpha(k, i) = [1 - \sum_{j=1}^{k-1} p(k, j, \tau_{OSR}(i, k))] \frac{b}{r_k[\tau_{OH} + \tau_{OSR}(i, k)]} \tag{7}$$

where b denotes the length[2] of a data packet, τ_{OH} denotes the constant overhead (e.g., RTS in IEEE 802.11 MAC protocol), in units of time, when initiating a packet transmission and $\tau_{OSR}(i, k)$ accounts for the remaining transmission time. A detailed explanation of $\tau_{OSR}(i, k)$ is included in Section IV-B.

C. Optimal Stopping Rules

We can now formally state the *stochastic decision problem* as follows: Given a forwarding node n_s which intends to forward a packet toward its destination and a set of L candidate relays $\{n_1, n_2, \ldots, n_L\}$ known at the routing layer, which can be characterized by L independent discrete random variables $\{\Theta_1, \Theta_2, \ldots, \Theta_L\}$ defined by (4), what is the optimal policy at the forwarding node n_s to select the relay to which the packet is to be forwarded so as to maximize the expected reward $E\{Y\}$?

This problem is an L-horizon optimal stopping problem which can be solved by the method of backward induction [9]. Regardless of implementation, we can divide the conceptual sequential observations into stages. Since we must stop at stage L, we first find the optimal policy at stage $L-1$. Then, given the optimal policy at stage $L-1$, we find the optimal policy at stage $L-2$ and so on back to the initial stage.

[2]We assume fixed-size packets and thus b is a constant throughout the paper.

Therefore, we define value functions at a forwarding node as follows. When $i = L$,

$$V_L^L(\theta_1, \theta_2, \ldots, \theta_L) = y_L(\theta_1, \theta_2, \ldots, \theta_L) = \theta_L \alpha(f(\frac{\theta_L}{d_L}), L) \tag{8}$$

then inductively for $i = L-1$ backward to $i = 1$,

$$V_i^L = \max\{y_i(\theta_1, \theta_2, \ldots, \theta_i), E\{V_{i+1}^L(\theta_1, \theta_2, \theta_i, \Theta_{i+1}) | \Theta_1 = \theta_1, \Theta_2 = \theta_2, \ldots, \Theta_i = \theta_i)\}\} \tag{9}$$

where V_i^L is short for $V_i^L(\theta_1, \theta_2, \ldots, \theta_i)$. Notice that V_i^L represents the maximum expected reward achieved by the forwarding node n_s starting from the stage i and having observed the random variables $\Theta_1 = \theta_1, \Theta_2 = \theta_2, \ldots, \Theta_i = \theta_i$.

Now we derive the optimal policy (OSR) from (8) and (9). Recall that different fading channels are mutually independent, $\{\Theta_1, \Theta_2, \ldots, \Theta_L\}$ for the set of candidate relays are independent as well, which implies that V_i^L only depends on Θ_i and $T_{L-i} = E\{V_{i+1}^L(\theta_1, \theta_2, \theta_i, \Theta_{i+1}) | \Theta_1 = \theta_1, \Theta_2 = \theta_2, \ldots, \Theta_i = \theta_i)\}$, which is a constant only depending on $L - i$, the number of stages to go. Thus, the optimal policy for the forwarding node n_s is to select the i-th candidate relay if $Y_i(\theta_1, \theta_2, \ldots, \Theta_i) = \Theta_i \alpha(\frac{\Theta_i}{d_i}, i) \geq T_{L-i}$, where T_{L-i} can be computed inductively as follows:

$$T_0 = -\infty \tag{10}$$

$$T_1 = E\{\Theta_L \alpha(f(\frac{\Theta_L}{d_L}), L)\} = \sum_{k=2}^{K} \pi_k^L d_L r_k \alpha(k, L) \tag{11}$$

$$\begin{aligned} T_{i+1} &= E\{\max\{\Theta_{L-i}\alpha(f(\frac{\Theta_{L-i}}{d_{L-i}}), L-i), T_i\}\} \\ &= \sum_{k=1}^{K} \pi_k^{L-i} \max\{d_{L-i} r_k \alpha(k, L-i), T_i\} \\ &= \sum_{k=2}^{K} \pi_k^{L-i} \max\{d_{L-i} r_k \alpha(k, L-i), T_i\} + \pi_1^{L-i} T_i \\ &, 1 \leq i \leq L-1 \end{aligned} \tag{12}$$

where π_k^j denotes the probability that the link of the j-th relay is in state s_k.

It is easy to observe that the derived thresholds $T_0, T_1, \ldots, T_{L-1}$ in the optimal policy form a non-decreasing sequence and T_L (i.e., $E\{V_1^L\}$) gives the expected reward $E\{Y\}$ achieved by the forwarding node n_s under the optimal policy.

IV. Optimal Stopping Relaying Implementation

A. Candidate Relays Selection in GPSR Protocol

OSR is implemented here assuming GPSR protocol provides the set of candidate relays. Notice that to avoid progress to be negative when selecting a node as the candidate relay, the selection procedure here is only considered for the greedy forwarding mode.

Let M denote a system parameter specifying the maximum order of spatial diversity in the network. In general, GPSR protocol returns top L ($\leq M$) candidate relays in terms of $\overline{\theta}_i$ (where $\overline{\theta}_i \approx E\{\Theta_i\}$). To obtain these metrics, apart from assuming that every node has the common knowledge of SNR thresholds from the FSMC model, progresses d_i and average channel SNR's $\overline{\gamma}_i$ are needed. Therefore, the forwarding node resorts to the location service to estimate the progresses d_i by acquiring locations of its neighbor and the destination nodes. Moreover, by setting its radio in the promiscuous mode, the forwarding node estimates the average channel SNR $\overline{\gamma}_i$ of its neighbor node n_i through an Exponentially Weighted Moving Average (EWMA) filter as in [22] with $\delta = 0.1$ using $\overline{\gamma}_i = (1-\delta)\overline{\gamma}_i + \delta\gamma_i$, where γ_i is the SNR measurement on the latest received/overheard packet from node n_i and $\overline{\gamma}_i$ is the estimated average SNR for node n_i by the forwarding node.

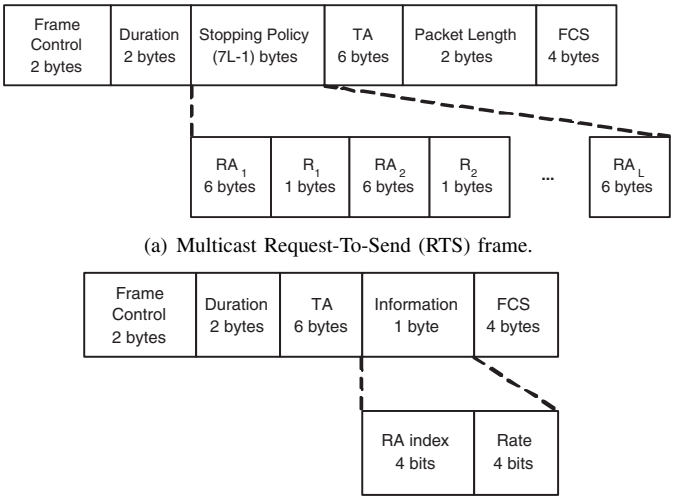

(a) Multicast Request-To-Send (RTS) frame.

(b) Clear-To-Send (CTS) frame.

Fig. 1. MAC frame formats used by OSR.

B. The Next-Hop Selection via a MAC Layer Anycast Scheme

When there is more than one candidate relays, the forwarding node uses a MAC layer anycast scheme, implemented here as an extension of IEEE 802.11 MAC DCF, to perform the optimal policy. The policy parameters, i.e., the thresholds as computed in subsection III-C, are contained in the multi-cast RTS (MRTS) frame, as shown in Fig. 1(a). In contrast to the standard RTS frame, an MRTS frame carries additional $L-1$ node addresses (6 bytes), $L-1$ thresholds (1 byte) and two bytes for the length (payload) of the packet to be forwarded.[3] In order to minimize the size of the MRTS frame, we do not include the destination address. Instead, we replace the threshold T_{L-i} by an encoded data rate as R_i satisfying $d_i R_i \alpha(f(R_i), i) \geq T_{L-i}$. Thereby, alleviating the need for computing the progress toward the destination, a candidate relay only needs to determine whether the observed channel state can support the data rate specified in the MRTS frame. The reply message, the CTS frame, is shown in Fig. 1(b). The CTS frame here is different from the standard CTS frame in that it carries one additional information byte. The upper four bits specify the index of the relay that replies in the list presented in the MRTS frame while the lower four bits encode the data rate supported by the selected relay.

Now we describe the MAC layer anycast scheme. When a node seizes the medium and intends to forward a packet toward its destination, it first multi-casts an MRTS frame to the set of candidate relays selected by the GPSR protocol. Upon reception of an MRTS frame, a candidate relay completes a channel measurement and accesses the received policy information to obtain its threshold. To decide whether to be "the selected relay," it compares the threshold with the highest reliable data rate supported by the measured channel state. In case more than one node qualifies under the policy, it needs a mechanism to resolve the potential collisions. We implement a priority-based scheme for resolution here since the number of candidate relays would not be large in exploiting spatial diversity in wireless ad hoc networks and collision detection cost in delay would be at least $\tau_{SIFS} + \tau_{PLCP} + \tau_{CTS}$ (See Table I). Specifically, the CTS reply frames are prioritized in time in the same order as specified in the MRTS frame: if the i-th candidate relay is qualified in that its maximum supported data rate $r_i \geq R_i$, it encodes (i, r_i) into the additional information byte and then schedules the transmission of its CTS frame after a period equal to $\tau_{SIFS} + (i-1)\tau_\sigma$. Notice that any frame sent by a candidate relay will reach all other relays with high probability within a slot time τ_σ since it the carrier sensing range

[3]In OSR, there is no threshold associated with the last relay since the forwarding node would select the last one anyway as long as its channel does not undergo deep fading (i.e., state s_1).

is commonly set to be two times of the transmission range at the base rate. This allows that a CTS frame scheduled by a relay will be suppressed if a CTS frame is sent by a relay with a higher priority. Next, when the forwarding node receives any CTS frame, it starts to transmit the DATA frame to the relay where this CTS frame comes from after a SIFS interval. Thus, when the i-th relay is selected, $\tau_{OSR}(i,k) = \tau_{dec}(i) + \tau_{tran}(k)$, where the decision-making time $\tau_{dec}(i) = \tau_{SIFS} + (i-1)\tau_\sigma + \tau_{PLCP} + \tau_{CTS} + \tau_{SIFS}$ and the remaining transmission time $\tau_{tran}(k) = \tau_{PLCP} + \tau_{DATA}(k) + \tau_{SIFS} + \tau_{PLCP} + \tau_{ACK}(k)$.[4] Finally, similar to the standard DCF, the DATA frame will be acknowledged by an ACK frame shortly after. Notice that the MRTS and CTS frames are transmitted at the base data rate while the DATA and ACK frames are transmitted at the data rate specified by the replied relay – this is typical of rate-adaptive MAC protocols (e.g., [23]).

To take advantage of rate adaptation on the DATA/ACK frame and avoid medium reservation in the MRTS frame (e.g., in [23]), we modify the Virtual Carrier Sensing (VCS) scheme in IEEE 802.11 MAC DCF as follows. Each frame attempts to reserve the medium only for the immediate next frame instead of reserving the medium for all remaining frames. Thereby, any node, except the node which actually replies with a CTS frame, overhearing the MRTS frame, sets its Network Allocation Vector (NAV) to $\tau_{SIFS}+(L-1)\tau_\sigma+\tau_{PLCP}+\tau_{CTS}$, the maximum time needed to wait for response from any next-hop relay. Any node that overhears a CTS frame sets its NAV to $\tau_{SIFS}+\tau_{PLCP}+\tau_{DATA}$, where τ_{DATA} is calculated based on the "Packet Length" field in the MRTS frame and the data rate indicated by the selected relay itself. Any node that overhears the DATA or ACK frame updates its NAV as usual (i.e., $\tau_{SIFS}+\tau_{PLCP}+\tau_{ACK}$ or zero).

Notice that in IEEE 802.11 MAC any node that initiates a usage of wireless medium will defer by a τ_{DIFS} which is longer than τ_{SIFS}, so all nodes that may potentially interfere on the ongoing frame exchange sequence can also defer properly depending on Physical Carrier Sensing (PCS). Even if all frames cannot be overheard clearly as assumed above, we can resort to τ_{EIFS} by setting it as $\tau_{SIFS} + (M-1)\tau_\sigma + \tau_{PLCP} + \max\{\tau_{CTS}, \tau_{ACK}\} + \tau_{DIFS}$, which is long enough for the transmission of any control frame. For example, when a node detects an erroneous frame corresponding to the MRTS frame, it will defer by an EIFS interval, which is large enough to allow the CTS frame to go through. This is also true when a node detects an erroneous frame corresponding to the DATA or ACK frame. Moreover, it is possible that some candidate relay does not receive the MRTS frame let alone possibly respond via a CTS frame due to a deep fading channel. In the worst case, if none of the CTS frames are received, the forwarding node goes into a random back-off and then retries.

Fig. 2 illustrates an example of using the proposed anycast extension based on the IEEE 802.11 MAC DCF modifications just described. Specifically, the time-line of a sample scenario begins with the forwarding node multi-casting an MRTS frame to its three candidate relays. The first relay withdraws its response since it is not qualified due to an unfavorable channel. The second relay is qualified and schedules a CTS frame at the time $\tau_{SIFS}+\tau_\sigma$ after reception of the MRTS frame. Regardless of the state of the underlying channel, the third relay schedules a CTS frame with a $\tau_{SIFS}+2\tau_\sigma$ interval later as long as it receives the MRTS frame. However, it is then suppressed by the second relay's CTS frame sent τ_σ earlier. The remaining events are similar to the standard DCF: when receiving a CTS frame, the forwarding node transmits the DATA frame to the second relay and then receives an ACK frame from it later on.

V. Performance Analysis of the Forwarding Capability of a Single Node

In this section, we first analyze the forwarding capability of a single node in FSR and LSR, respectively. Then we numerically compare their achieved expected rewards with that of OSR under various network settings. Notice that all derived analytical and numerical results in this section represent upper bounds of these schemes since we do not consider collisions or erroneously detected frames with EIFS deferral as discussed in Section IV-B.

[4] $\tau_{DATA}(k)$ is defined as $\frac{b}{r_k}$. The similar applies to $\tau_{ACK}(k)$.

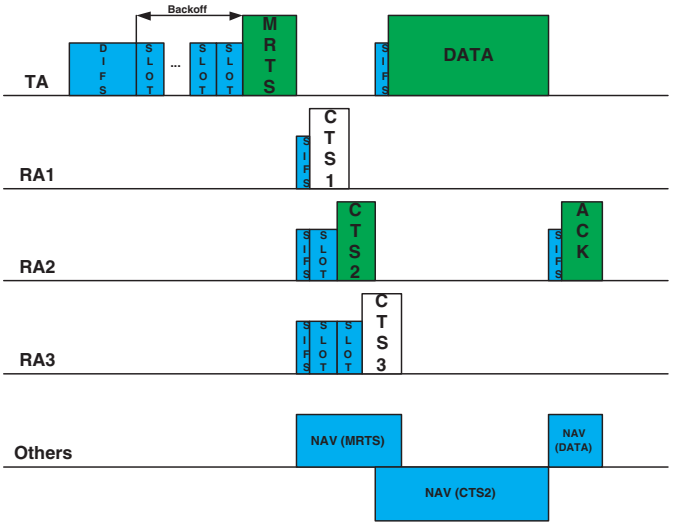

Fig. 2. A sample timeline of the OSR scheme for three candidate nodes.

A. First Stopping Relaying

We assume that FSR shares the same implementation as OSR, described in Section IV, except that in FSR any next-hop relay is qualified as long as it receives the MRTS frame.[5] As a result, the forwarding node always selects the first relay that replies. In order to evaluate the expected reward achieved by a forwarding node via FSR, we first calculate the probability that the i-th ($1 \le i \le L$) candidate relay is selected as follows.

$$p^i = \prod_{j=1}^{i-1} \pi_1^j (1-\pi_1^i). \tag{13}$$

Next, let I be a random variable for the selection of the i-th candidate relay. Then the PMF of I can be expressed as

$$I = \begin{cases} i & \text{w.p. } p^i,\ 1 \le i \le L \\ 0 & \text{w.p. } 1-\sum_{i=1}^{L} p^i = \prod_{j=1}^{L} \pi_1^j \end{cases} \tag{14}$$

Now, the expected reward given that the i-th candidate relay is selected can be calculated as

$$\begin{aligned} E\{Y|I=i\} &= \sum_{k=2}^{K} Pr\{R=r_k|I=i\} d_i r_k \alpha(k,i) \\ &= \sum_{k=2}^{K} \frac{\pi_k^i}{1-\pi_1^i} d_i r_k \alpha(k,i). \end{aligned} \tag{15}$$

Finally, to sum up all cases, the expected reward for a forwarding node in FSR is

$$\begin{aligned} E\{Y\} = E\{E\{Y|I\}\} &= \sum_{i=1}^{L} Pr\{I=i\} E\{Y|I=i\} \\ &= \sum_{i=1}^{L} \prod_{j=1}^{i-1} \pi_1^j d_i \sum_{k=2}^{K} \pi_k^i r_k \alpha(k,i). \end{aligned} \tag{16}$$

[5] Notice that the MRTS frame in FSR does not have threshold fields.

B. Last Stopping Relaying

We assume that LSR shares the same implementation as channel-adaptive relaying in [6], except that LSR uses the IE metric defined in (4). Therefore, the forwarding node always selects the i-th candidate relay that satisfies $i = \arg\max_{1\le i\le L}\{\Theta_1, \Theta_2, \ldots, \Theta_L\}$. Notice that the node uniformly makes its random decision if there are multiple qualified relays. In order to evaluate the expected reward achieved by a forwarding node via LSR, we first derive the probability distribution of Θ_i $(1 \le i \le L)$ as follows.

Without loss of generality, we assume that the set V contains all possible values that can be taken by Θ for all candidate relays.[6] With (4), the Cumulative Distribution Function (CDF) of Θ_i is

$$\begin{aligned} Pr\{\Theta_i \le v\} &= Pr\{d_i R_k \le v\} \\ &= \sum_{k:d_i r_k \le v} \pi_k^i,\ k \in \{1, 2, \ldots, K\},\ v \in V \end{aligned} \tag{17}$$

Next, let $\Theta \triangleq \max\{\Theta_1, \Theta_2, \ldots, \Theta_L\}$. Recall $\{R_i\}$ are independent and $\{d_i\}$ are constants, $\{\Theta_i\}$ are independent as well. Therefore, the CDF of Θ is

$$\begin{aligned} Pr\{\Theta \le v\} &= Pr\{\max\{\Theta_1, \Theta_2, \ldots, \Theta_L\} \le v\} \\ &= Pr\{\Theta_1 \le v, \Theta_2 \le v, \ldots, \Theta_L \le v\} \\ &= Pr\{\Theta_1 \le v\} Pr\{\Theta_2 \le v\} \ldots Pr\{\Theta_L \le v\} \\ &= \prod_{i=1}^{L} \Big(\sum_{k:d_i r_k \le v} \pi_k^i \Big). \end{aligned} \tag{18}$$

Then, the PMF of Θ is

$$Pr\{\Theta = v_n\} = Pr\{\Theta \le v_n\} - Pr\{\Theta \le v_{n-1}\} \tag{19}$$

where v_{n-1} is the largest element of V less than v_n.

Finally, the expected reward for a forwarding node in LSR is

$$E\{Y\} = \sum_{v_n \in V} v_n \beta(f(\frac{v_n}{d_i})) Pr\{\Theta = v_n\} \tag{20}$$

where the discount factor $\beta(k)(\in [0, 1])$ for LSR is similarly defined as

$$\beta(k) = [1 - \sum_{j=1}^{k-1} p(k, j, \tau_{LSR}(k))] \frac{b}{r_k[\tau_{OH} + \tau_{LSR}(k)]} \tag{21}$$

where $\tau_{LSR}(k) = \tau'_{dec} + \tau_{tran}(k)$ with $\tau'_{dec} = \tau_{SIFS} + L(\tau_{PLCP} + \tau_{CTS'} + \tau_{SIFS})$[7] and $\tau_{tran}(k) = \tau_{PLCP} + \tau_{DATA}(k) + \tau_{SIFS} + \tau_{PLCP} + \tau_{ACK}(k)$ (refer to [5, Fig. 5][8]).

In a special case where $\{\Theta_i\}$ are i.i.d. and $\{d_i\}$ are equal as d, eq. (19) can be simplified as

$$\begin{aligned} Pr\{\Theta = v_n\} &= \prod_{i=1}^{L} \Big(\sum_{k:d_i r_k \le v_n} \pi_k^i \Big) - \prod_{i=1}^{L} \Big(\sum_{k:d_i r_k \le v_{n-1}} \pi_k^i \Big) \\ &= \Big(\sum_{k=1}^{n} \pi_k\Big)^L - \Big(\sum_{k=1}^{n-1} \pi_k\Big)^L \end{aligned} \tag{22}$$

where $v_n = dr_n$ $(1 \le n \le K)$ and $\{\pi_k^i\}$ are equal to π_k $(1 \le n \le K)$ due to the above i.i.d. assumption.

Accordingly, eq. (20) becomes

$$E\{Y\} = \sum_{n=1}^{K} dr_n \beta(r_n) \Big[\Big(\sum_{k=1}^{n} \pi_k\Big)^L - \Big(\sum_{k=1}^{n-1} \pi_k\Big)^L\Big]. \tag{23}$$

[6]At a time scale of per-packet transmission, since $\{d_i\}$ can be approximated as constants, together with the fact that a radio only provides finite discrete rates, V can be quantified as a finite set.

[7]Notice that, while the time between receipt of the CTS of the selected relay and receipt of the ACK should be the function of the selected relay, the time between channel measurement on the relay side (i.e., when receiving the MRTS) until the forwarding node utilizes these measured channel state information is a constant. As a result, the decision-making time τ'_{dec} in LSR is independent of the selected relay, which is different from OSR and FSR.

[8]In [5], the modified CTS frame is 36 bytes in length.

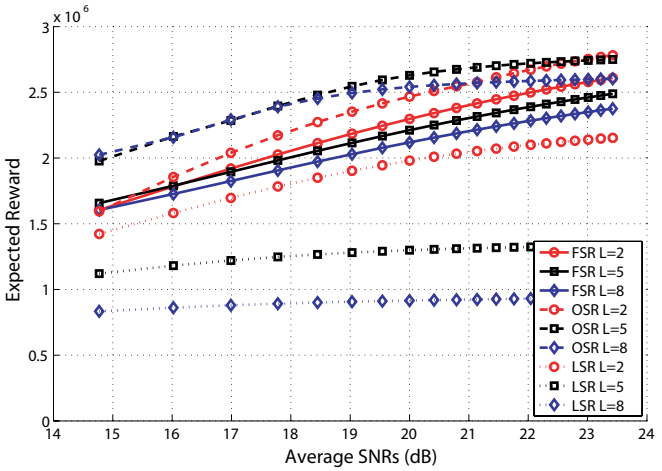

Fig. 3. The expected reward achieved by FSR, OSR and LSR v.s. the average SNRs when maximum fading velocity is set to be 1 m/s (b=512 bytes).

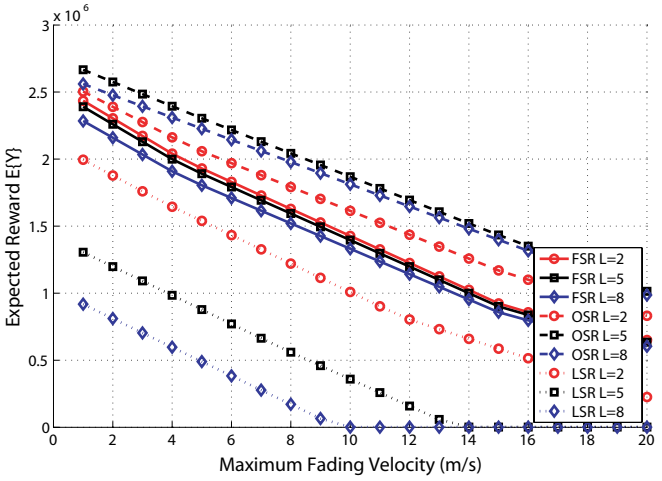

Fig. 4. The expected reward achieved by FSR, OSR and LSR v.s. maximum fading velocity when the average SNRs are set to be 120 (b=512 bytes).

C. Numerical Results

We here compare the forwarding capability of a single node for FSR, OSR and LSR in terms of the expected reward achieved. In the following evaluations, we assume that every node deploys an 802.11b compatible radio in which the SNR thresholds in the FSMC model are properly set and the corresponding set of data rates are $\{2, 5.5, 11\}$ Mbps.[9] Without loss of generality, we further assume that there are exactly L candidate relays for the forwarding node with unit progresses toward its destination and i.i.d. channels.

To evaluate the impact of channel qualities, Fig. 3 shows the expected reward achieved by FSR, OSR and LSR as a function of the average SNRs when maximum fading velocity is set to be 1 m/s.[10] As expected, all schemes with any given L always achieve higher expected reward with the increase of average SNRs. On the other hand, for any given L, the expected reward achieved by OSR is higher than that of FSR (up to $7.67\%, 20.99\%, 26.15\%$ for $L = 2, 5, 8$) due to its *optimized* decision rule and the expected reward achieved by LSR is lower than that of both OSR and FSR (up to $29.13\%, 105.88\%, 178.21\%$, for $L = 2, 5, 8$) mainly due to its relatively low $\frac{\tau_{DATA}}{\tau}$ in the discount factor. However, for any

[9]SNR thresholds are calculated from the radio reception sensitivities for the corresponding modulation schemes under Additive White Gaussian Noise (AWGN) channel assumption.

[10]For simplicity, we vary the transmission power to simulate the change of average channel SNRs instead of altering the distance.

TABLE I
PARAMETERS IN MAC ANYCAST SCHEME BASED ON IEEE 802.11B DCF

τ_σ	20 μs
τ_{SIFS}	10 μs
τ_{DIFS}	50 μs
τ_{PLCP}	192 μs
RTS	$15 + 7L$ bytes
CTS	15 bytes
ACK	14 bytes

given scheme, the patterns of achieved expected reward on L are quite different. For LSR, the larger the L, the lower the expected reward for any given average SNR, which indicates that the spatial diversity gain induced by a larger L is completely overwhelmed by $\frac{\tau_{DATA}}{\tau}$ in the discount factor. For FSR, when $L > 5$, the pattern is similar to LSR as the channel probing overhead incurred by a larger L completely negates the spatial diversity gain for any given average SNR. However, when $L \leq 5$, a larger L always leads to higher expected reward in the low SNR regime (e.g., $SNR < 16dB$) while the opposite is true in the high SNR regime. This exemplifies the role of L on tuning the trade-off between spatial diversity and channel probing overhead. Finally, for OSR, its performance pattern is very similar to FSR in every aspect except reaching a better trade-off. For example, when in the low SNR regime (e.g., $SNR < 16dB$), OSR still achieves higher expected reward with a larger L even beyond $L = 5$, though negligible. Moreover, when $L \leq 5$, it is generally true that a larger L gives higher expected reward, though the gaps diminish with the increase of average SNR. Thus, OSR reaps more spatial diversity gain over a wider range of average SNRs than FSR.

To evaluate the impact of channel variations, Fig. 4 plots the expected reward achieved by FSR, OSR and LSR as a function of the maximum fading velocity when the average SNRs are set to be 120 ($\approx 20.79dB$). As expected, all schemes with any L always achieve lower expected reward with the increase of maximum fading velocity. On the other hand, for any given L, the decreasing rate of the expected reward achieved by OSR is less than that of FSR, and similarly for FSR compared to LSR. Furthermore, when $L \geq 3$ (not shown in Fig. 4), the expected reward achieved by LSR will fall on a "floor" (almost three orders less than that of the slow-fading case) beyond certain maximum fading velocity, implying the transmission time with channel probing overhead of a packet is larger than channel coherence time with high probability.

VI. END-TO-END PERFORMANCE EVALUATION

A. Simulation Model

In this section, we compare the end-to-end performance of OSR with FSR and LSR in QualNet 3.7 [14] simulation environment. The common simulation settings are as follows. Routing layer uses GPSR protocol with average beacon interval of 1.5 seconds. MAC layer uses the anycast extension of IEEE 802.11 MAC DCF described in Section IV-B and its detailed parameters are listed in Table I. The physical layer uses IEEE 802.11b supporting multiple data rates (i.e., 2/5.5/11 Mbps). The radio transmission power is 4.145 dBm, resulting a 1024-byte packet delivery probability of 0.9 when the receiver is 250 m away from the transmitter. The radio reception sensitivities are -83.0 dBm (11 Mbps), -87.0 dBm (5.5 Mbps), -89.0 dBm (2 Mbps) and -93.0 dBm (carrier sense), respectively. The antenna for each node is omnidirectional and the propagation is modeled as a combination of two-ray path loss and time-varying correlated fading.

B. Grid Topology, A Single FTP Flow

We first evaluate end-to-end throughput of FSR, OSR and LSR in the following setting: a 10×10 grid topology where nodes are 100 m apart, a single File Transfer Protocol (FTP) session transmits 512-byte data packets from the node 12 (located in the upper-left corner) to the node 89 (located in the down-right corner). Starting at the 20th second, the file transfer ends when $5,000$ data packets are successfully delivered.

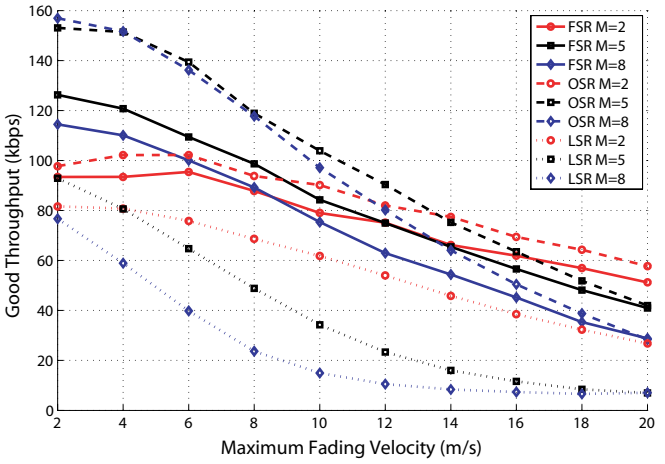

Fig. 5. Good FTP throughput vs. maximum fading velocity for 10×10 grid topology with Rayleigh fading.

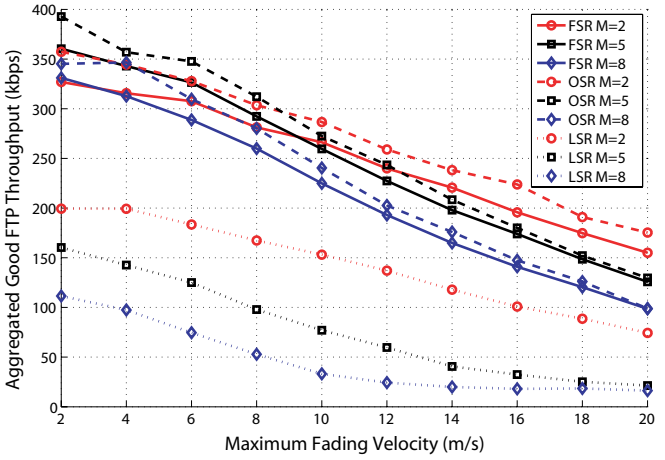

Fig. 6. Aggregated FTP goodput vs. maximum fading velocity for random topology with Rayleigh fading.

Fig. 5 depicts the FTP goodput of FSR, OSR and LSR with $M = 2, 5, 8$ as a function of maximum fading velocity v_m.[11] Similar to our numerical results in Section V-C, LSR achieves the least throughput compared to both FSR and OSR with any set of parameters (i.e., M and v_m). Furthermore, we observe the following trends in the performance of LSR, FSR and OSR.

LSR achieves less throughput with a larger M for any given v_m except when $v_m < 4$ m/s. This again demonstrates that the channel probing overhead incurred by LSR is critical for negating the spatial diversity gain.

FSR achieves its largest throughput when $M = 5$, higher than that achieved when $M = 8$ and $M = 2$ given $v_m < 8$ m/s; this is because the $M = 2$ case does not achieve enough spatial diversity gain while the $M = 8$ case incurs *extra* channel probing overhead. However, with further increase of v_m, FSR achieves its largest throughput when $M = 2$ eventually, higher than the case $M = 5$ and $M = 8$, which can be well explained by taking the upper layer TCP mechanism into account; any spatial diversity relaying scheme inevitably introduces out-of-order delivery at the destination node which will trigger fast retransmission at the source node intending to recover the packet loss immediately. Nonetheless, out-of-order delivery is usually wrongly interpreted by TCP in wireless environments since most of packets

[11] In practice, depending on application scenarios, it is reasonable to estimate v_m that used for threshold calculation in our OSR scheme.

thought to be "lost" are actually on their way to be delivered. On the other hand, due to the deteriorated channels with the increase of v_m, more packets are kept from being delivered during a given interval, also triggering more timeout events at the source node. Consequently, more redundant packets are injected into the network, which results in network congestion and TCP performance degradation. By inspecting the simulation trace files, it is confirmed that a larger M usually triggers fast retransmission more frequently and thus explains our observation.

Finally, for the case of OSR, its behavior is very similar to FSR in every aspect except that such a "turning point" appears at a higher v_m. Furthermore, for any given M, OSR always achieves larger throughput than that of FSR due to its optimized decision policy given any v_m. For example, when $M = 2$, even with only two decision choices, OSR still achieves 10.59% (up to 17.04%) more throughput than FSR in average; when $M = 5$ and $M = 8$, OSR achieves 17.56% (up to 27.42%) and 23.68% (up to 37.77%) more throughput than FSR in average, respectively. Nevertheless, it is also observed that the throughput gap between OSR and FSR for any given M diminishes with the increase of v_m. It can also be explained as that the better spatial diversity relaying capability causes a higher probability of out-of-order delivery which in turn degrades TCP performance.

C. Random Topology, Multiple FTP Flows

We here evaluate the impact of multiple flows on end-to-end throughput of FSR, OSR and LSR in the following setting: rather than regular topology as above, 100 nodes are randomly and uniformly deployed in a $1,200 \times 1,200$ m^2 square area; five FTP sessions transmits 512-byte data packets between five disjoint source and destination pairs. Starting at the 20th second, the simulation ends when each session successfully delivers $1,000$ data packets.

Fig. 6 plots the aggregated FTP goodput of FSR, OSR and LSR with $M = 2, 5, 8$ as a function of the maximum fading velocity v_m.[12] The drawn results show almost the same pattern as the single FTP flow case, except that the throughput gains of OSR over FSR decrease. For example, when $M = 2$, OSR achieves 9.33% (up to 14.31%) more throughput than FSR on average; when $M = 5$ and $M = 8$, OSR achieves 5.27% (up to 9.00%) and 5.83% (up to 10.82%) more throughput than FSR on average, respectively. The reason is that, the heavier traffic causes more spatial blocking caused by MAC-layer anycast scheme among packet transmission sessions. It potentially decreases the spatial diversity gain to be exploited, especially by OSR, which assumes that all intended candidate relays are available in advance.

D. Mobile Topologies, Multiple CBR Flows

We finally evaluate the impact of traffic load and mobility on the *packet delivery ratio* (PDR) and end-to-end delay of FSR, OSR and LSR. In the first part of evaluation, the network is set as follows: 200 nodes are randomly and uniformly deployed in a $3,000 \times 600$ m^2 rectangle area; maximum fading velocity v_m is fixed at 5 m/s; accordingly, the node mobility model follows the random way-point mobility model with zero pause time and speeds selected from the interval $(0, 5]$ m/s; we vary the traffic load in terms of the number of Constant Bit Rate (CBR) flows from 2 to 20 with disjoint source and destination pairs; each flow generates 512-byte data packets at the rate of 5 packets/s. Starting at the 20th second, the simulation ends until each session delivers $1,000$ data packets.

Fig. 7(a) plots the PDR of FSR, OSR and LSR with $M = 2, 5, 8$ as a function of the number of CBR flows. LSR achieves the least PDR compared to both FSR and OSR with any set of parameters and in general it achieves less PDR with a larger M. Moreover, due to its largest channel probing overhead, even when the number of CBR flows grows beyond six, PDRs of LSR with any M drop sharply and then stabilize around some value less than 10%. Comparatively, PDRs of FSR or OSR drop gracefully with the increase of the number of CBR flows: it achieves the best PDR when $M = 5$, while $M = 8$ and $M = 2$ achieve lower PDRs, which follows the same pattern as our numerical results shown in subsection V-C. On the other hand, for any given M, OSR achieves a larger PDR than that of FSR at any v_m. For example, when $M = 2$, OSR achieves 10.47% (up to 52.62%) more PDR than FSR in average; when $M = 5$ and $M = 8$, OSR achieves 9.96% (up to 45.43%) and 11.74% (up to 54.66%) more PDR than FSR in average. Moreover, average end-to-end delay shown in Fig. 7(b) follows a similar pattern as Fig. 7(a).[13] For example, when $M = 2$, OSR achieves 17.68% (up to 50.64%) less end-to-end delay than FSR in average; when $M = 5$ and $M = 8$, OSR achieves 24.03% (up to 51.54%) and 29.29% (up to 54.65%) less end-to-end delay than FSR in average.

Next, in the second part of evaluation, inheriting the above network setting, we fix the number of CBR flows to 10 but vary the maximum fading velocity and corresponding maximum node speed. Fig. 8(a) plots the PDR of FSR, OSR and LSR with $M = 2, 5, 8$ as a function of maximum fading velocity. LSR achieves the least PDR compared to both FSR and OSR with any set of parameters. Moreover, when the maximum fading velocity ranges from 2 to 20 m/s, its PDRs are always around some value below 0.3 and it always achieves the best PDRs with $M = 2$ and then $M = 5$ and $M = 8$. On the other hand, PDRs of FSR or OSR drop gracefully with the increase of v_m and show a similar pattern when varying M: when v_m is small, it again achieves the best PDRs with $M = 5$, with $M = 8$ and $M = 2$ achieving lower PDRs; while beyond some v_m, it achieves its best PDRs with $M = 2$ instead of $M = 5$ since the channel probing overhead starts to overwhelm the spatial diversity gain when v_m is large. For any given M, OSR achieves a larger PDR than that of FSR at any v_m. For example, when $M = 2$, OSR achieves 4.18% (up to 9.42%) more PDR than FSR in average; when $M = 5$ and $M = 8$, OSR achieves 5.58% (up to 15.01%) and 6.66% (up to 18.52%) more PDR than FSR in average, respectively. Once more, the average end-to-end delay shown in Fig. 8(b) follows a similar pattern as Fig. 8(a). For example, when $M = 2$, OSR achieves 12.32% (up to 21.91%) less end-to-end delay than FSR in average; when $M = 5$ and $M = 8$, OSR achieves 21.19% (up to 37.99%) and 22.93% (up to 31.06%) less end-to-end delay than FSR in average, respectively.

VII. Conclusions

In this paper, we formulated the next-hop spatial-diversity selection problem as a sequential optimal decision problem in a stochastic decision framework. Hence, we derived an Optimal Stopping Relaying (OSR) policy for improving spatial diversity gain in wireless ad hoc networks. Compared to previous schemes, the key difference is that OSR optimizes the selection of the next-hop in terms of arbitrary channel-related metric based on optimal stopping theory while minimizing the channel probing overhead. Assuming Rayleigh fading channels, we implemented this policy with the link adaptation scheme to optimize a generalized information efficiency (IE) metric in a protocol stack composed of Greedy Perimeter Stateless Routing (GPSR) and IEEE 802.11 MAC. The performance evaluation was conducted from two aspects. First, we analytically compared the forwarding capability of a single node of First Stopping Relaying (FSR), OSR and Last Stopping Relaying (LSR) in terms of the achieved expected reward. Owing to incurring less channel probing overhead, OSR and FSR outperforms LSR. Moreover, owing to intelligently skipping non-optimal next-hop relays, OSR outperforms FSR. Second, we evaluated the end-to-end performance of these three schemes via extensive simulations in QualNet. The simulation results show that OSR provides better services to upper layer applications (i.e., FTP, CBR) than the other two schemes. Thereby, both the mathematical and simulation studies show that OSR achieves the best trade-off between the channel selection and channel probing overhead, which can be attributed to its underlying optimal stopping

[12]Each data point is averaged over five independent realizations of a topology/mobility pattern. The same follows in the remaining experiments.

[13]Due to the relatively poor PDR, average end-to-end delays achieved by LSR are several orders higher than both FSR and OSR and thus omitted. The same applies in Fig. 8(b) as well.

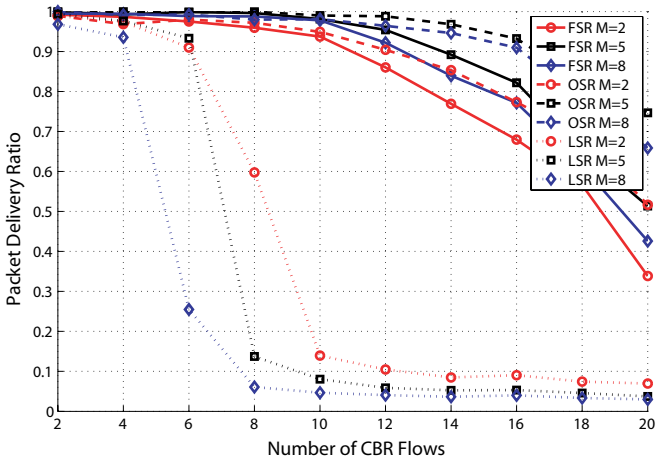

(a) Average packet delivery ratio.

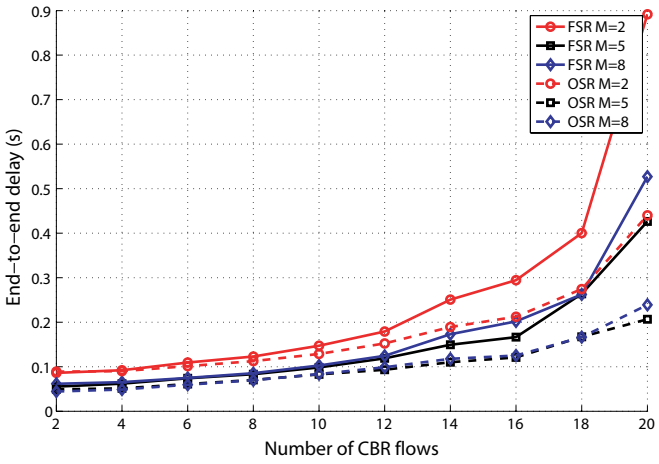

(b) Average end-to-end delay.

Fig. 7. End-to-end performance of FSR, OSR and LSR vs. the number of CBR flows for mobile topologies with Rayleigh fading $v_m = 5$ m/s.

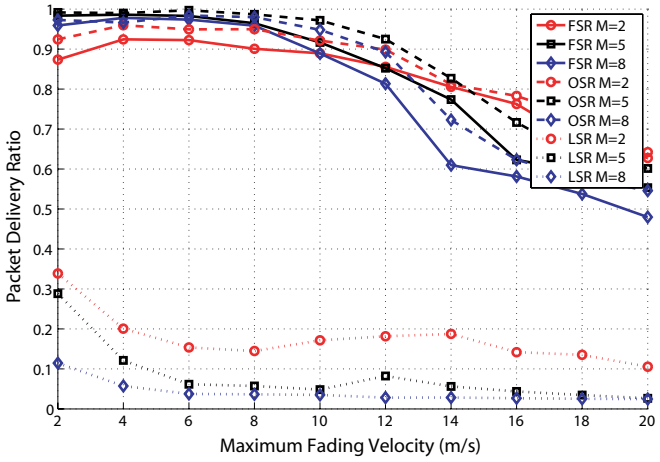

(a) Average packet delivery ratio.

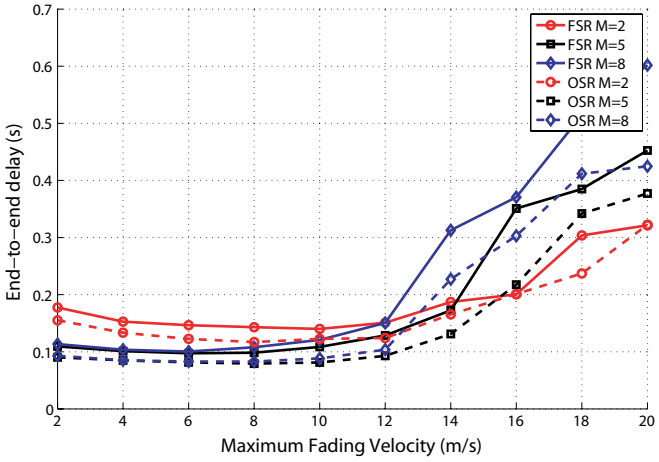

(b) Average end-to-end delay.

Fig. 8. End-to-end performance of FSR, OSR and LSR vs. maximum (fading) velocity for mobile topologies with Rayleigh fading by setting the number of CBR flows to be 10.

theory and efficient implementation that utilizes the broadcast nature of the wireless medium.

Finally, it is worth noting that we do not explicitly consider interference in design of spatial diversity relaying schemes in this paper. Specifically, we assumed that the carrier sensing range is twice of the transmission range, and resorted to RTS/CTS scheme in IEEE 802.11 MAC protocol to mitigate interference. OSR achieved remarkable spatial diversity gain in the observed simulations and mathematical analysis. Nevertheless, interference management in networks with high interference should be taken into consideration and it is the subject of future study.

APPENDIX
DERIVATION OF (2)

In [17], [18], authors derive the transition probabilities from state s_k to state s_j after a time interval τ as

$$p(k,j,\tau) \approx \begin{cases} \frac{N(\gamma_j)}{\pi_k}\tau & \text{if } j = k+1 \\ \frac{N(\gamma_{j+1})}{\pi_k}\tau & \text{if } j = k-1 \\ 1 - \sum_{i \neq k} p(k,i,\tau) & \text{if } j = k \end{cases} \tag{24}$$

We can observe that, in (24), it requires that $|k-j| \leq 1$. In order to remove such a constraint, we extend the above results as follows. For example, assuming $j > k$, we aggregate state $s_k, s_{k+1} \ldots, s_{j-1}$ as a new state $s_{k'}$. Thereby, the transition probability between those two neighbor states is

$$p(k', j, \tau) = \frac{N(\gamma_j)}{\pi'_k}\tau \tag{25}$$

where $\pi_{k'} = \sum_{i=k}^{j-1} \pi_i$. On the other hand, given the initial aggregated state $s_{k'}$, the probability that the refined initial state to be s_k is $\frac{\pi_k}{\pi_{k'}}$. Combined the above results, we have

$$\begin{aligned} p(k,j,\tau) &= p(k',j,\tau)\frac{\pi_k}{\pi_{k'}} \\ &= \frac{N(\gamma_j)}{\sum_{i=k}^{j-1}\pi_i}\frac{\pi_k}{\sum_{i=k}^{j-1}\pi_i}\tau. \end{aligned} \tag{26}$$

Following the above approach, we can reach the same results in the other two branches in (2).

ACKNOWLEDGEMENT

The authors would like to thank Dr. Souryal of National Institute of Standards and Technology for providing the source codes used in [5]. They are also grateful to Dr. R. Berry and the anonymous reviewers for their valuable suggestions which helped improving the quality and presentation of this paper. This work was supported in part by National Science Foundation (NSF) grant No. ANI-0546402.

REFERENCES

[1] J. Ai, A. A. Abouzeid, and Z. Ye, "Cross-layer optimal decision policies for spatial diversity relaying in wireless ad hoc networks," in *Proc. IEEE MASS*, Vancouver, Canada, Oct. 2006.

[2] R. R. Choudhury and N. H. Vaidya, "Mac-layer anycasting in ad hoc networks," *ACM SIGCOMM Computer Communun. Rev.*, vol. 34, pp. 75–80, 2004.

[3] J. Wang, H. Zhai, and Y. Fang, "Reliable and efficient packet forwarding by utilizing path diversity in wireless ad hoc networks," in *Proc. IEEE MILCOM*, vol. 1, Monterey, CA, USA, Nov. 2004, pp. 258–264.

[4] S. Jain and S. R. Das, "Exploiting path diversity in the link layer in wireless ad hoc networks," in *Proc. IEEE WoWMoM*, Taormina, Italy, June 2005, pp. 22–30.

[5] M. R. Souryal and N. Moayeri, "Channel-adaptive relaying in mobile ad hoc networks with fading," in *Proc. IEEE SECON*, Santa Clara, CA, USA, Sept. 2005, pp. 142–152.

[6] ——, "Joint rate adaptation and channel-adaptive relaying in 802.11 ad hoc networks," in *Proc. IEEE MILCOM*, Washington, DC, USA, Oct. 2006.

[7] R. Knopp and P. Humblet, "Information capacity and power control in a single cell multiuser environment," in *Proc. IEEE ICC*, vol. 1, Seattle, WA, USA, June 1995, pp. 331–335.

[8] T. S. Rappapport, *Wireless Communications: Principles and Practise*, 2nd ed. Prentice Hall, 2002.

[9] T. S. Ferguson, "Optimal stopping and applications." [Online]. Available: http://www.math.ucla.edu/ tom/Stopping/Contents.html

[10] X. Qin and R. Berry, "Opportunistic splitting algorithms for wireless networks," in *Proc. IEEE INFOCOM*, vol. 3, HongKong, China, Mar. 2004, pp. 1662–1672.

[11] M. W. Subbarao and B. L. Hughes, "Optimal transmission ranges and code rates for frequency-hop packetradio networks," *IEEE Trans. Commun.*, vol. 48, pp. 670–678, 2000.

[12] P. Bose, P. Morin, I. Stojmenovic, and J. Urrutia, "Routing with guaranteed delivery in ad hoc wireless networks," in *Proc. ACM DIALM*, Seattle, WA, USA, Aug. 1999, pp. 48–55.

[13] B. Karp and H. T. Kung, "Gpsr: greedy perimeter stateless routing for wireless networks," in *Proc. ACM/IEEE MOBICOM*, Boston, MA, USA, Aug. 2000, pp. 243–254.

[14] "Qualnet 3.7 user's guide." [Online]. Available: http://www.scalable-networks.com/

[15] V. Kanodia, A. Sabharwal, and E. W. Knightly, "Moar: a multi-channel opportunistic auto-rate media access protocol for ad hoc networks," in *Proc. IEEE BROADNETS*, San Jose, CA, USA, Oct. 2004, pp. 600–610.

[16] S. Biswas and R. Morris, "Exor: opportunistic multi-hop routing for wireless networks," in *Proc. ACM SIGCOMM*, Philadelphia, PA, USA, Aug. 2005, pp. 133–144.

[17] H. Wang and N. Moayeri, "Finite-state markov channel - a useful model for radio communications channels," *IEEE Trans. Veh. Technol.*, vol. 43, pp. 163–171, 1995.

[18] Q. Zhang and S. A. Kassam, "Finite-state markov model for rayleigh fading channels," *IEEE Trans. Commun.*, vol. 47, pp. 1688–1692, 1999.

[19] P. Larsson, "Selection diversity forwarding in a multihop packet radio network with fading channel and capture," in *Proc. ACM MOBIHOC*, vol. 5, Long Beach, CA, USA, Oct. 2001, pp. 47–54.

[20] M. Zorzi and R. R. Rao, "Geographic random forwarding (geraf) for ad hoc and sensor networks: multihop performance," *IEEE Trans. Mobile Computing*, vol. 2, pp. 337–348, 2003.

[21] M. R. Souryal, B. R. Vojcic, and R. L. Pickholtz, "Information efficiency of multihop packet radio networks with channel-adaptive routing," *IEEE J. Select. Areas Commun.*, vol. 23, pp. 40–50, Jan. 2005.

[22] Z. Ji, Y. Yang, J. Zhou, M. Takai, and R. Bagrodia, "Exploiting medium access diversity in rate adaptive wireless lans," in *Proc. ACM/IEEE MOBICOM*, Philadelphia, PA, USA, 2004, pp. 345–359.

[23] G. Holland, N. Vaidya, and P. Bahl, "A rate-adaptive mac protocol for multi-hop wireless networks," in *Proc. ACM/IEEE MOBICOM*, Rome, Italy, July 2001, pp. 236–251.

Jing Ai (S'05) received his B.E. and M.E. in the Electrical Engineering from Huazhong University of Science and Technology (HUST) in 2000 and 2002, respectively. He is completing his Ph.D. degree in the Department of Electrical, Computer, and Systems Engineering at Rensselaer Polytechnic Institute. He defensed his doctoral dissertation in June, 2008 and will join Juniper Networks in August, 2008. His research interests include coverage and connectivity in wireless sensor networks, dynamic resource allocation, stochastic scheduling and cross-layer design in various types of wireless networks, e.g., wireless ad hoc networks, cognitive radio networks. He is a student member of IEEE.

Alhussein A. Abouzeid received the B.S. degree with honors from Cairo University, Cairo, Egypt in 1993, and the M.S. and Ph.D. degrees from University of Washington, Seattle, WA in 1999 and 2001, respectively, all in electrical engineering.

From 1993 to 1994 he was with the Information Technology Institute, Information and Decision Support Center, The Cabinet of Egypt, where he received a degree in information technology.

From 1994 to 1997, he was a Project Manager in Alcatel telecom.

He held visiting appointments with the aerospace division of AlliedSignal (currently Honeywell), Redmond, WA, and Hughes Research Laboratories, Malibu, CA, in 1999 and 2000, respectively.

He is currently Associate Professor of Electrical, Computer, and Systems Engineering, and Deputy Director of the Center for Pervasive Computing and Networking, Rensselaer Polytechnic Institute (RPI), Troy, NY.

His research interests span various aspects of computer networks. He is a recipient of the Faculty Early Career Development Award (CAREER) from the US National Science Foundation in 2006. He is a member of IEEE and ACM and has served on several technical program and executive committees of various conferences. He is also a member of the editorial board of Computer Networks (Elsevier).

Zhenzhen Ye (S'07) received the B.E. degree from Southeast University, Nanjing, China, in 2000, the M.S. degree in high performance computation from National University of Singapore, Singapore, in 2003, and the M.S. degree in electrical engineering from University of California, Riverside, CA in 2005. He is currently working towards the Ph.D. degree in electrical engineering in Rensselaer Polytechnic Institute, Troy, NY.

His research interests lie in the areas of wireless communications and networking, including stochastic control and optimization for wireless networks, cooperative communications in mobile ad hoc networks and wireless sensor networks, and ultra-wideband communications.